

Research on a Scroll Expander Used for Recovering Work in a Fuel Cell

Gao Xiaojun, Li Liansheng, Zhao Yuanyang, Shu Pengcheng
National Engineering Research Center of Fluid Machinery & Compressors,
School of Energy and Power Engineering,
Xi'an Jiaotong University, Xi'an 710049, P.R. China
Tel: 86-29-82675393; Fax: 86-29-83237910, 82663792
gxjabc@sohu.com

Shen, Jiang
Tianjin Commercial University,
Tianjin 300134, P.R. China

Abstract

The energy of the exhausted high-pressure air from a proton exchange membrane (PEM) fuel cell can still be recovered. The performance of the scroll expander used for recovering this energy is studied in this paper. A numerical simulation of the expander is presented, and then the simulated results are compared with that of the experiment results gleaned from the prototype of the expander. The matching of the flows and pressure characteristics between the compressor-expander (C-E) is also discussed. Finally, this paper points out that leakage has a significant effect on the volumetric efficiency, the quantity of recovered work, and other performance indicators of the scroll expander. The matching of the C-E is a key factor in the practical application of this system.

Keywords: Fuel cell, scroll expander, work recovery, compressor-expander matching

1. Introduction

1.1 Fuel cell

A fuel cell is an electrochemical device that converts the chemical energy of a fuel (e.g., hydrogen) and an oxidant (e.g., O₂) into electrical energy continuously. Because the reaction does not involve combustion, the net electrical efficiency of the fuel cell system is not limited by the "Carnot cycle" and can reach 40% to 60% (W. He, 1998). Moreover, pollutant emissions to the environment can be significantly reduced. The fuel cell also has the feature of low noise, high reliability, and easy maintenance. Furthermore, the fuel cell is appropriate for a wide range of applications. Hence, as a novel technology, the fuel cell has drawn the interest of people all over the world.

Fuel cells can be broadly classified into five types: Alkaline (AFC), Solid Oxide (SOFC), Molten Carbonate (MCFC), Phosphoric Acid (PAFC) and Proton Exchange Membrane (PEM) (Cownden and Nahon, 2001). Among these types,

the PEM fuel cell is a likely candidate for light-duty vehicles, buildings, and potentially for much smaller applications such as a replacement for rechargeable batteries due to its high-energy conversion ratio, low operating temperature, high power density, and adaptability in the case of frequent start-up.

In practical applications, the fuel cell often works under above-atmospheric pressure conditions. Hence it needs a compressor system to supply air. In the fuel cell stack, the pressure drop of compressed air is only about 0.05MPa (Yuanyang and Liansheng, 2003). The exhausted air, thus, still has a considerable amount of energy due to its elevated pressure. An expander can be used to recover this energy and the recovered work can be provided to the compressor, which shares the same shaft with the expander. In this way, the actual power consumption of the compressor can be reduced and the efficiency of the fuel cell system improved. The fuel cell system considered here is shown in *Figure 1*.

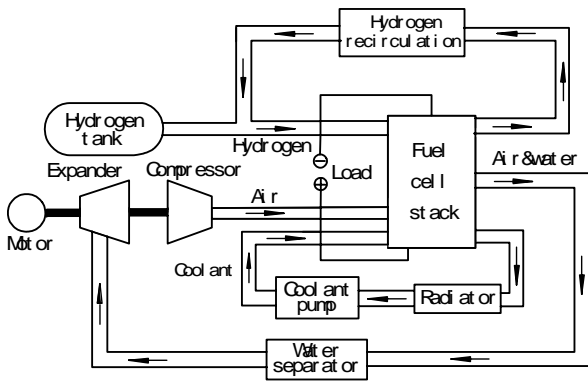


Figure 1. Fuel cell system.

1.2 Basic working principle of the scroll expander

The scroll expander consists of a pair of scrolls called fixed and orbiting scrolls, respectively. The two scrolls, whose axes of rotation do not match together, are assembled at a relative angle of 180°. The expander process includes three phases: charging, expansion and discharging. The charging phase begins at an orbiting angle of 0°, when the air starts to enter the charging chambers. The charging chambers are sealed when $\theta = \theta_s$, and then the air in the expansion chambers starts to be expanded. When the orbiting angle is equal to the discharge angle θ_d , the chambers open up to the discharge region and begin to discharge. The working principle of the scrolls is shown in Figure 2.

During the expansion process, the air pushes the center of orbiting scroll to go around the center of the fixed scroll, and there is output work delivered through the eccentric shaft.

2. Numerical Simulation of the Expander Process

2.1 Basic assumptions

- (1) The expanded air can be regarded as an ideal gas at all times, and the parameters of the air in the control volume are uniform;
- (2) The heat exchange between the air and the walls is ignored, and the expander process is regarded as an isentropic one;
- (3) The suction pressure and the discharge pressure are constant;
- (4) The porting during the charging process is ignored.

2.2 Energy equation

A pocket is taken as the control volume. The kinetic energy and the potential energy of the air flowing in and out of the control volume are ignored. Based on the conservation of energy and of mass, the following energy balance is found:

$$d(\mu) = dQ + \sum h_i dm_i - \sum h_o dm_o + dW \quad (1)$$

Using the assumption that the flow from the control volume is an instantaneous and stable process, we can set $h = h_c$. Additionally, $h = C_p T$, $dQ = 0$, $dW = -PdV_c$, and equation (1) becomes

$$d(\mu) = -PdV_c + C_p \sum T_i d(m_i) - C_p T \sum d(m_o) \quad (2)$$

According to $\theta = \omega t$, equation (2) can be rewritten as follows:

$$\frac{dT}{d\theta} = -\frac{(k-1)T}{V_c} \frac{dV_c}{d\theta} + \frac{K}{m} \left(K \frac{T_i}{T} - 1 \right) \frac{dm_i}{d\theta} - \frac{(k-1)T}{m} \frac{dm_o}{d\theta} \quad (3)$$

2.3 Leakage equation

There are two types of leakage in the scroll expander. One is radial leakage, which goes through a clearance between the bottom (or the top) plate and the scrolls. The other is flank leakage, which goes through a clearance between the flanks of two scrolls. The clearances are illustrated in Figure 3. According to the nozzle leakage model, the radial leakage can be expressed by (Liansheng, 1998)

$$\frac{dm_{ri}}{d\theta} = -\frac{a_r \rho_i(\theta) c_r L_r(\theta)}{\omega} \cdot \sqrt{\frac{2K}{K-1} R T_i(\theta) \left[1 - \left(\frac{P_{i+1}(\theta)}{P_i(\theta)} \right)^{\frac{K-1}{K}} \right]} \quad (4)$$

The flank leakage is given by

$$\frac{dm_{ri}}{d\theta} = -\frac{a_r \rho_i(\theta) c_r h}{\omega} \cdot \sqrt{\frac{2K}{K-1} R T_i(\theta) \left[1 - \left(\frac{P_{i+1}(\theta)}{P_i(\theta)} \right)^{\frac{K-1}{K}} \right]} \quad (5)$$

while the change of mass in the control volume can be calculated as follows:

$$dm_i = dm_{li} + dm_{ri} \quad (6)$$

$$dm_o = dm_{lo} + dm_{ro} \quad (7)$$

All the working parameters of the expander can be found by solving equations (3) to (7).

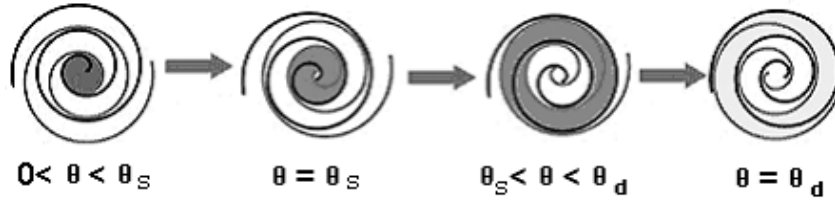


Figure 2. Working principle of the scrolls.

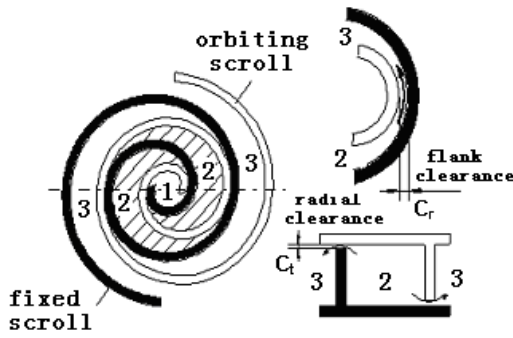


Figure 3. Radial and flank leakage model.

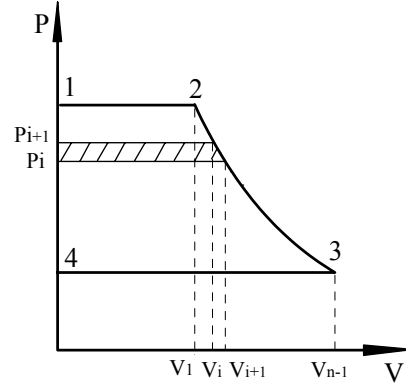


Figure 4. Expander process.

3. Performance Parameters

3.1 Theoretical expansion ratio, ρ

When the number of the expansion pockets (n) is an integer, the expression of expansion ratio is given by

$$\rho = [(2n - 1)/(1 + \theta_s/\pi)]^K \quad (8)$$

or it is calculated by

$$\rho = [(2N - 1 - \theta^*/\pi)/(1 + \theta_s/\pi)]^K \quad (9)$$

where $N = \text{int}(n) + 1$, $\theta^* = 2\pi [1 - (n - \text{int}(n))]$ and $\text{int}(n)$ is the nearest round-off of n .

3.2 Delivery Q

The delivery Q is a very important parameter for a scroll expander. In this paper, it is calculated by accumulating the net mass of air entering the control volume each time interval.

3.3 Indicated work W_i

The indicated work of the scroll expander is given by (shown graphically in Figure 4)

$$W_i = \frac{1}{2} \sum_{i=1}^n (V_{i+1} + V_i)(P_{i+1} - P_i) \quad (10)$$

W_i is delivered by the air in the control volume during the expander process. Using the pocket number and rotating speed, one can find the indicated work of the expander.

3.4 Indicated isentropic efficiency η_{ie} and isentropic efficiency η_e

To evaluate the performance of an expander under different working conditions, a set of criteria should be employed. For the expander used in the fuel cell, it is reasonable to appraise the expander by the volumetric efficiency η_v and by η_{ie} and η_e . Here η_{ie} is defined as

$$\eta_{ie} = \frac{W_i}{W_e} \quad (11)$$

where W_e is the work of the ideal expansion process. There is no resistance loss and porting loss during the charging and discharging processes and the over and deficient expansions do not occur, although they exist in the practical process. W_e is calculated by

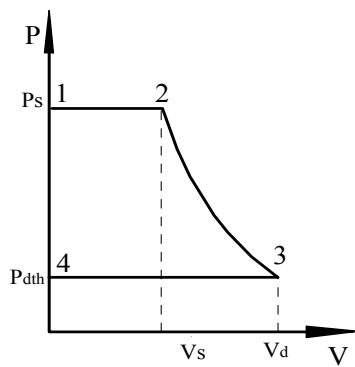
$$W_e = \frac{K}{K-1} V_s P_s \left[1 - \left(\frac{P_d}{P_s} \right)^{\frac{K-1}{K}} \right] \quad (12)$$

Taking into account the mechanical losses, the isentropic efficiency η_e can be found as follows:

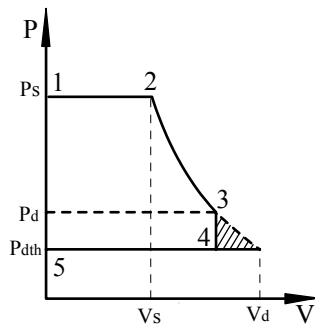
$$\eta_e = \eta_{ie} \cdot \eta_m = \frac{W_i - W_f}{W_e} \quad (13)$$

In the simulation, the mechanical efficiency $\eta_m = 0.80$. There are many factors affecting the parameter η_e . The following are the primary ones.

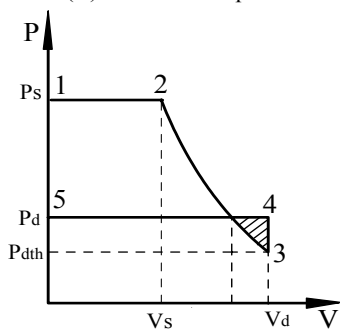
First, the charging pressure is lower than the nominal suction pressure due to the existence of flow loss and porting loss. Second, the pressure after expansion is not exactly equal to the discharge pressure. When it is higher than the discharge pressure, an isochoric expansion loss will occur; and when it is lower than the discharge pressure, the gas in the discharge pocket will flow backward into the control volume and an isochoric compression loss will appear. The hatched area shown in *Figure 5* denotes the energy loss. Third, leakage exists during the whole process. All these factors result in a reduction of the isentropic efficiency.



(A) normal expansion



(B) deficient expansion



(C) over expansion

Figure 5. Three types of expansion.

3.5 Volumetric efficiency η_v

The volumetric efficiency is an important

parameter used to assess the performance of the expander and is defined as the ratio of theoretical delivery to the practical delivery as follows (Ziwen, 1993):

$$\eta_v = \frac{V_{th}}{V_s} \quad (12)$$

V_{th} is the volume of the control volume when the charging phase has just finished and the rotation angle is 0° . There are two primary factors affecting the volumetric efficiency. One is the leakage that adds to the quantity of the air consumed by the expander. The other is porting, which makes the charging pressure lower than the nominal suction pressure and results in a reduction of the air entering the expander. When the effect of porting exceeds that of leakage, η_v is greater than 100%. Otherwise η_v is below 100%.

4. Prototype of expander and test system

4.1 Prototype of expander

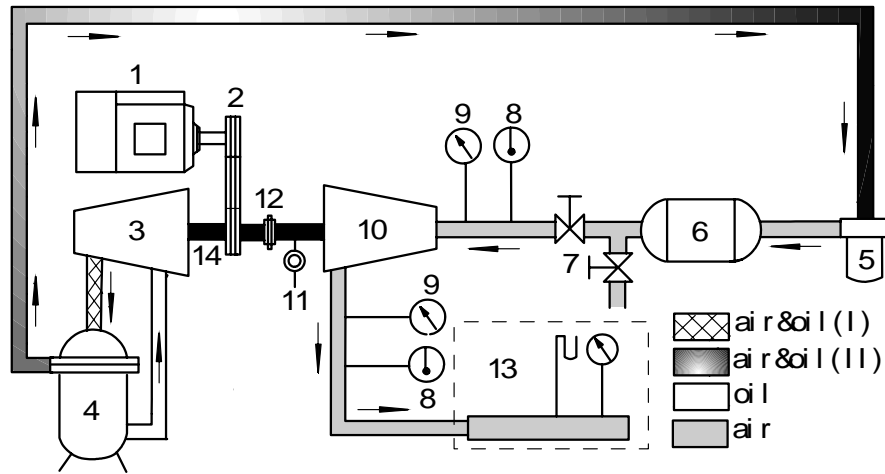
A prototype expander was designed and fabricated by the National Engineering Research Center (NERC) for Fluid Machinery & Compressors at Xi'an Jiaotong University. The wrap type is the involutes of a circle. The starting part of the involutes is revised with a PMP curve. The material of the scroll parts of the prototype is a titanium alloy while the basic parameters of the scroll are shown in TABLE I.

TABLE I. THE BASIC PARAMETERS OF THE SCROLL EXPANDER.

Radius of basic circle (a)	6.05 mm
Scroll pitch (P)	38 mm
Scroll height (h)	60 mm
Scroll width (t)	7 mm
Charging volume (V_{th})	0.0004 m ³
Radial clearance	0.015mm
Expansion pockets (n)	2
Initial angle of involutes (α)	33.15°
Initial expansion angle (θ^*)	240°
Radius of eccentric shaft (r)	12 mm
Flank clearance	0.01mm

4.2 Test principle and system

The test system is shown in *Figure 6*. The expander is directly coupled with the compressor by an elastic connection so that the compressor can be driven well. However, to begin with, the compressor is not coupled with the expander and is driven by a motor and operates with a rotating speed of n . The discharge pressure is then adjusted to P and the electric power (N_1) consum-



- | | | | | |
|----------------|------------------------|-----------------------------|----------------------|----------------------|
| 1. motor | 2. belt | 3. compressor | 4. oil separator(I) | 5. oil separator(II) |
| 6. gas tank | 7. valve | 8. thermometer | 9. manometer | 10. expander |
| 11. tachometer | 12. elastic connection | 13. delivery measure system | 14. concentric shaft | |

Figure 6. Test system of the expander.

ed by the compressor is recorded. Next, the compressor, connected to the expander and still driven by the motor, operates with the same rotating speed n and discharge pressure P . The electric power consumption (N_2) is measured. N (calculated by $N_1 - N_2$) can approximately be regarded as the output work of the expander. The delivery, the pressure, and the temperature of the air flowing in and out of the expander are also measured.

5. Analysis of the Numerical Simulation Results

Figures 7 to 11 show the results of the numerical simulation with different rotating speeds and charging pressures. Figure 7 presents the relationship between the expansion ratio and rotating speed for different charging pressures. When the charging pressure is 2, 3 and 4 bar, the expansion ratio decreases as the rotating speed increases but is higher than the design ratio 1.764. The expansion ratios are correlated with charging pressures at low rotating speed due to the leakage in the process. The lower the charging pressure is, the lower the ratio becomes. However, when the rotating speed goes up to a certain value all the curves become flat, which means that the ratios become independent of the charging pressures at high rotating speeds. It can also be seen that the ratio becomes small and below 1.764 when the charging pressure drops to 1.5 bar, which causes the over-expansion during the process. There is an approximately linear relationship between delivery and rotating speed (shown in Figure 8).

We can see from Figure 9 that the indicated isentropic efficiency becomes a little larger as the

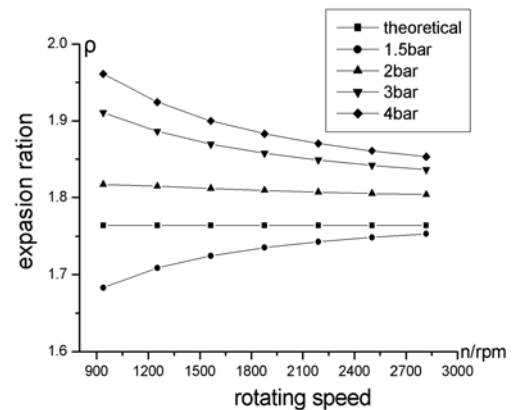


Figure 7. Expansion ratio.

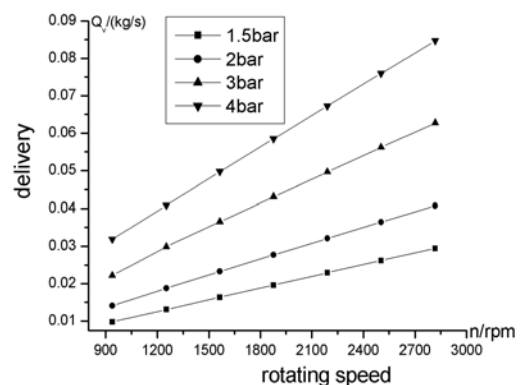


Figure 8. Delivery of the expander.

rotating speed increases but decreases when the charging pressure goes up. However, when the charging pressure is 1.5 bar and an over expansion occurs in the process, the 1.5 bar curve is below that for 2 bar.

Now, since the porting is ignored in our

study, the volumetric efficiency is below 1 (shown in *Figure 10*). It can be seen that the volumetric efficiency increases as the rotating speed increases, changes more quickly at low rotating speeds, and becomes more stable at high rotating speeds. The reason for this may be that the leakage is larger at the low rotating speeds than at the higher ones.

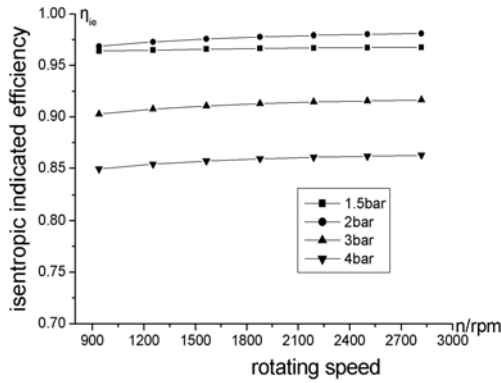


Figure 9. Indicated isentropic efficiency.

The relationship between the leakage rate and the rotation angle for different charging pressures and rotating speeds is shown in *Figure 11*. From this figure one can see that every curve has a jump at a rotation angle of 210° . The reason is that the expansion pocket opens up to the discharging region and the leakage mode changes at this angle.

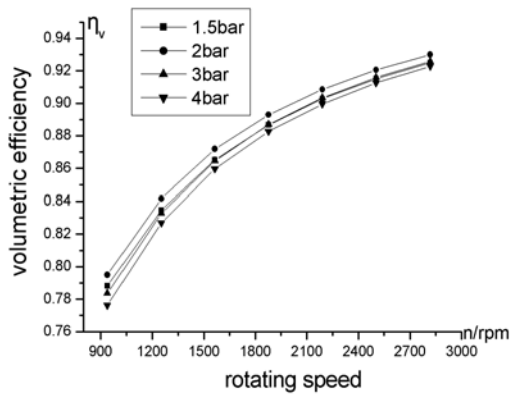
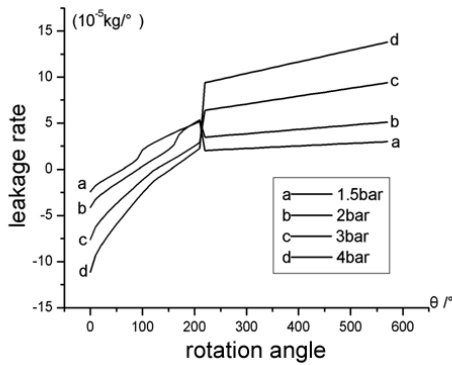
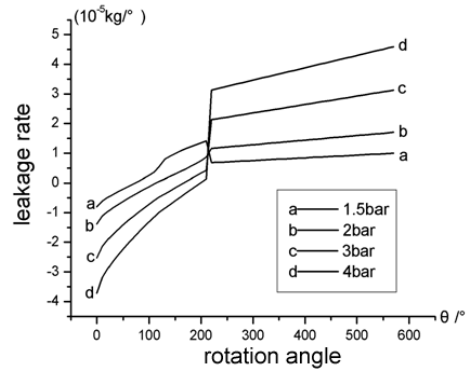


Figure 10. Volumetric efficiency.



(a) $n=939 \text{ rpm}$



(b) $n=2817 \text{ rpm}$

Figure 11. Leakage rate.

6. Experimental Results and Analysis

The electric power N_1 consumed by the compressor working alone is shown in *Figure 12* and the power N_2 consumed by the compressor-expander can be seen in *Figure 13*. The differential value of N_1 and N_2 can approximately be regarded as the output work of expander (shown in *Figure 15*). *Figure 14* shows the theoretical output work of the expander.

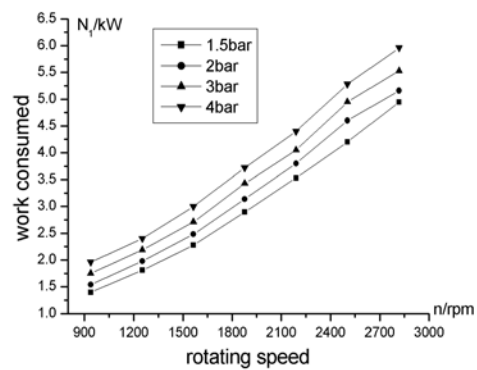


Figure 12. Electric power consumed by compressor.

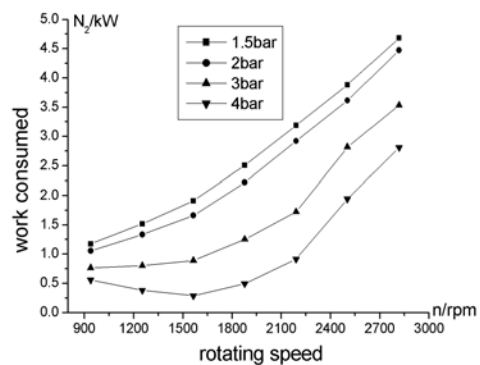


Figure 13. Electric power consumed by the C-E.

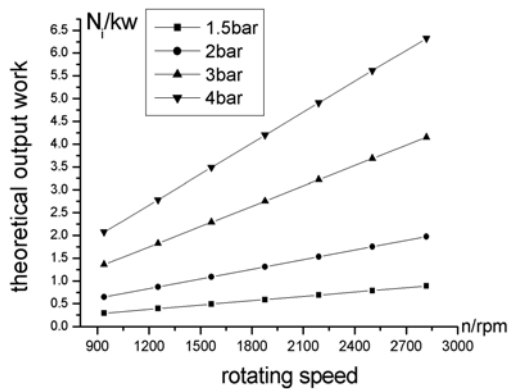


Figure 14. Theoretical expander output work.

We can see from Figure 14 that the theoretical output work of the expander increases as the rotating speed and charging pressure increase. However, in our study, there is an optimum rotating speed, corresponding to each charging pressure, at which the output work is a maximum. The optimum rotating speed falls with a drop in charging pressure, which can be seen in Figure 15. The primary reason is that the increase

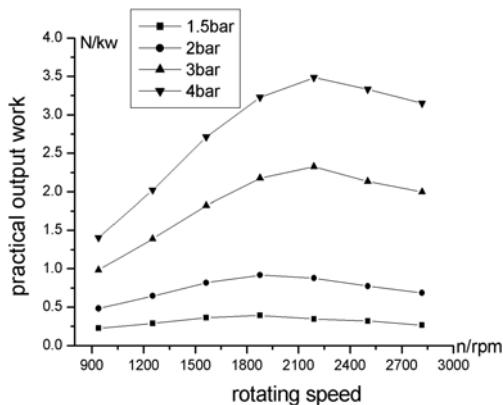


Figure 15. Practical expander output work.

in rotating speed leads to a deterioration of the lubricating condition of the expander and an enlargement of the mechanical loss of the compressor-expander system. From Figure 8 we can conclude that the delivery becomes larger when the rotating speed goes up, while on the other hand, the output work of the expander goes down after the optimum rotating speed is reached. Thus, the design rotating speed should be lower than the optimum value.

7. Matching of the C-E

The scroll expander used in the fuel cell is connected with the compressor. Their rotating speeds are the same. To make the C-E system work properly and efficiently, their flow, pressure

and other working parameters must match each other. Recently, Xiaojun (2004) developed expressions for determining whether or not the compressor and the expander match each other. As we know, the fuel cell often works under differing load conditions, especially in vehicular applications. The flow, the pressure, the force, and the power consumed by the compressor change frequently due to different loads on the fuel cell. All these changes influence the working parameters of the scroll expander. Thus, since the compressor and the expander may not match each other any more, measures have to be taken to adjust the working parameters of the expander. Usually there are two approaches to resolve this problem. When the flow is deficient, an auxiliary heat source is designed to change the inlet temperature of the gas to compensate for the volumetric flow decrease and add to the output work of the expander. The effectiveness of this approach is limited and other more effective means have to be adopted to compensate for the flow decrease. When the flow is excessive, a set of by-pass pipes is used to reduce the flow. Recently the NERC for Fluid Machinery & Compressors at Xi'an Jiaotong University presented other measures to resolve the matching problem by modifying the structure of the expander. One is to design a discharge valve to control the discharge angle and, thus, avoid over expansion appearing in the expansion process. The other is to design special components to change the suction volume of the expander, consequently adjusting its delivery. All in all, the matching of the C-E is a key factor in the practical application of this system.

8. Conclusions

In this paper, the operating properties of a scroll expander used for recovering energy were presented theoretically and experimentally. The study shows that leakage is a key element, which will significantly affect the volumetric efficiency, the quantity of recovered work, and other performance parameters. Furthermore, the practical output work of the expander, unlike the theoretical one, does not monotonically increase with an increase in rotating speed. Thus, there is an optimum rotating speed corresponding to each charge pressure at which the output work is a maximum. In addition, both deficient expansion and over expansion negatively affect the operating performance of the expander and reduce the output work of the expander, especially the over expansion. Not only does it add to the extra work, but it even deteriorates the operating condition of the expander.

Finally, the matching of operating parameters between the compressor and expander

is very important for the practical application of the C-E system.

Acknowledgements

The work described in the paper is funded by a key Research Project Fund of the Chinese Ministry of Education.

Nomenclature

a	flowing coefficient
c	average leakage clearance
C_p	specific heat at constant pressure
dm	mass change
dm_l	leakage mass
dQ	heat exchange through the boundary
h	enthalpy per unit mass
H	height of scrolls
K	isentropic coefficient
$L(\theta)$	length of leakage clearance
n	number of expansion pockets, rotational speed
P	pressure
Q	delivery
R	gas constant
T	temperature
u	internal energy per unit mass
V	instantaneous volume
W	Work
η	Efficiency
ρ	instantaneous density of the air
ω	angular speed of the expander shaft

Subscripts

c	control volume
d	Discharge

f	Friction
i	indicated, flowing into the control volume
ie	indicated isentropic
m	Mechanical
o	flowing out of the control volume
r	Radial
s	Suction
t	Axial
v	Volumetric

References

- Cownden, R., Nahon, M., 2001, "Exergy analysis of a fuel cell power system for transportation applications", *Exergy*, Vol.1, pp.112-121
- He, W., 1998, "Dynamic model for molten carbonate fuel cell power generation systems", *Energy Convers. Mgmt*, Vol.39, No.8, pp.775-783
- Liansheng, L., 1998, *Scroll compressor*, The mechanical industry press
- Xiaojun, G., 2004, "Simulation and Experiment Study on Scroll Expander Used in Fuel Cell", MSc Thesis, Xi'an Jiao Tong University.
- Yuanyang, Z., Liansheng, L., 2003, "Research on oil-free air scroll compressor with high speed in 30 kW fuel cell", *Applied Thermal Engineering*, Vol.23, pp.593-603
- Ziwen, X., 1993, "The characteristics of systems with rotary vane expander for converting low-grade heat into power", PhD Thesis, Xi'an Jiao Tong University